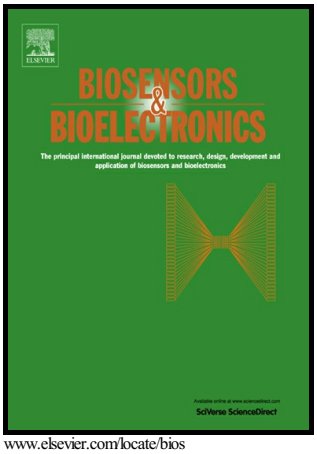

www.elsevier.com/locate/bios

Water-soluble mercury ion sensing based on the thymine-Hg^{2+}-thymine base pair using retroreflective Janus particle as an optical signaling probe

Hyeong Jin Chun, Saemi Kim, Yong Duk Han, Dong Woo Kim, Ka Ram Kim, Hyo-Sop Kim, Jae-Ho Kim, Hyun C. Yoon

PII: S0956-5663(18)30013-7
DOI: https://doi.org/10.1016/j.bios.2018.01.008
Reference: BIOS10201

To appear in: *Biosensors and Bioelectronic*

Received date: 26 October 2017
Revised date: 27 December 2017
Accepted date: 4 January 2018

Cite this article as: Hyeong Jin Chun, Saemi Kim, Yong Duk Han, Dong Woo Kim, Ka Ram Kim, Hyo-Sop Kim, Jae-Ho Kim and Hyun C. Yoon, Water-soluble mercury ion sensing based on the thymine-Hg^{2+}-thymine base pair using retroreflective Janus particle as an optical signaling probe, *Biosensors and Bioelectronic,* https://doi.org/10.1016/j.bios.2018.01.008

BIOS-D-17-03278R2, Revised manuscript

Water-soluble mercury ion sensing based on the thymine-Hg^{2+}-thymine base pair using retroreflective Janus particle as an optical signaling probe

Hyeong Jin Chun, Saemi Kim, Yong Duk Han, Dong Woo Kim, Ka Ram Kim, Hyo-Sop Kim, Jae-Ho Kim, Hyun C. Yoon*

Department of Molecular Science and Technology, Ajou University, Suwon 443749, South Korea

* Author to whom correspondence should be addressed:

E-mail: hcyoon@ajou.ac.kr

Abstract

Herein, we report an optical sensing platform for mercury ions (Hg^{2+}) in water based on the integration of Hg^{2+}-mediated thymine-thymine (T-T) stabilization, a biotinylated stem-loop DNA probe, and a streptavidin-modified retroreflective Janus particle (SA-RJP). Two oligonucleotide probes, including a stem-loop DNA probe and an assistant DNA probe, were utilized. In the absence of Hg^{2+}, the assistant DNA probe does not hybridize with the stem-loop probe due to their T-T mismatch, so the surface-immobilized stem-loop DNA probe remains a closed hairpin structure. In the presence of Hg^{2+}, the DNA forms a double-stranded structure with the loop region via Hg^{2+}-mediated T-T stabilization. This DNA hybridization induces stretching of the stem-loop DNA probe, exposing biotin. To translate these Hg^{2+}-mediated structural changes in DNA probe into measurable signal, SA-RJP, an optical signaling label, is applied to recognize the exposed biotin. The number of biospecifically bound SA-RJPs is proportional to the concentration of Hg^{2+}, so that the concentration of Hg^{2+} can be quantitatively analyzed by counting the number of RJPs. Using the system, a highly selective and sensitive measurement of Hg^{2+} was accomplished with a limit of detection of 0.027 nM. Considering the simplified optical instrumentation required for retroreflection-based RJP counting, RJP-assisted Hg^{2+} measurement can be accomplished in a much easier and inexpensive manner. Moreover, the detection of Hg^{2+} in real drinking water samples including tap and commercial bottled water was successfully carried out.

Keywords: Mercury ion sensing, Retroreflective Janus particles, Optical biosensor, Hg^{2+}-mediated thymine-thymine base pairing, Stem-loop DNA probe.

1. Introduction

The development of industry has created various types of environmental pollution factors. A particularly dangerous type of pollutant, heavy metals, can enter the body through respiration or cultivated crops, and cause many problems. In particular, long-term exposure to mercury can lead to conditions such as kidney failure and brain damage (Liu and Lu, 2007; Zhang et al., 2013). Water-soluble mercury ions (Hg^{2+}) are particularly capable of penetration into the body because they are the most stable form of mercury, and are widely distributed in soil, water, and the atmosphere (Miller et al., 1996). Therefore, it is very important to measure and analyze the Hg^{2+} present in an environment such as soil and water quickly, sensitively, and selectively. To date, many analytical techniques have been reported for the detection of Hg^{2+}, such as inductively coupled plasma mass spectrometry (ICP-MS) (Fong et al., 2007; Malinovsky et al., 2008), atomic absorption spectroscopy (AAS) (Bloom and Fitzgerald, 1988; Ferrua et al., 2007), and atomic fluorescence spectroscopy (AFS) (Li et al., 2009). Although these analytical techniques provide sensitive and precise measurements, they require expensive and sophisticated equipment with complicated sample preparation processes, making them unsuitable for simple use. To solve these problems, Hg^{2+} measurement methodologies using small organic molecules (Yang et al., 2005; Ros-Lis et al., 2005), functionalized polymer materials (Kim and Bunz, 2006), proteins (Wegner et al., 2007), and porphyrin compounds (Yang et al., 2009) have been studied. However, these sensing approaches also have limitations, such as low water solubility (Rurack et al., 2000), cross-sensitivity to other metal ions, and difficulty in the synthesis of probe materials. Therefore, there is an increasing need for the development of an efficient Hg^{2+} sensing system that is rapid, sensitive, selective, and simple to operate.

Recently, many Hg^{2+} measurement techniques using deoxyribonucleic acid (DNA) have been announced, in part because DNA is easy and inexpensive to produce, so it is a promising analytical reagent for the detection of Hg^{2+}. These properties were confirmed in 2004 by Ono and Togashi who measured Hg^{2+} concentration using DNA probes (Ono and Togashi, 2004). They first reported the property of Hg^{2+} that allows it to specifically bind two DNA thymine bases to form a stable thymine-Hg^{2+}-thymine (T-Hg^{2+}-T) pair. A thymine base, in general, forms DNA double helix structure by forming two hydrogen bonds with an adenine base, not with a thymine. However, when Hg^{2+} is present, a thymine base can pair with another thymine base through the mediation of Hg^{2+}. This Hg^{2+}-mediated base pair was found more stable than adenine-thymine pair (Li et al., 2006; Xiong et al., 2015; Wang et al., 2011). Ono and Togashi applied this property to fabricate a fluorescent Hg^{2+} detection sensor. In their sensor, a specifically designed single-stranded T-rich DNA, which is labeled with a fluorophore

and a quencher, would fold into a hairpin structure in the presence of Hg^{2+}, causing a reduction in fluorescence intensity by the fluorescence resonance energy transfer (FRET). Their sensor has a limit of detection (LOD) of 40 nM, higher than the upper limit for Hg^{2+} concentration in drinking water (10 nM) as prescribed by the United States Environmental Protection Agency (US-EPA) (US-EPA, 2001). However, when the single-stranded thymine-rich DNA was used for the detection of Hg^{2+}, it is considered to be a signal-off type sensor in which the signal decreases as the concentration of Hg^{2+} increases by FRET (Wang et al., 2011; Wang et al., 2015; He et al., 2012). This signal-off type sensor has a disadvantage in that the signal change cannot exceed 100% because it is observing a gradually decreasing amount of optical intensity from the maximum signal intensity (Yu and Lai, 2012; Xiong et al., 2015).

To overcome this limitation, a signal-on type optical-based Hg^{2+} sensor using a stem-loop DNA probe has been studied. A stem-loop DNA probe was labeled with a fluorophore and a quencher (Teh et al., 2014; Xu et al., 2011; Hou et al., 2012; Li et al., 2016). In the absence of Hg^{2+}, this DNA probe is present as a hairpin structure due to a stem region that has a complementary sequence. As the fluorophore and the quencher are located close to each other, the fluorescence signal is not observed. Conversely, when Hg^{2+} and the loop region complementary assistant DNA is present, the DNA probe of the hairpin structure is unfolded by the T-T mismatch, allowing the appearance of the fluorescence signal. The intensity of fluorescence increases in proportion to the concentration of Hg^{2+}, and the signal change can exceed 100%. These approaches using the fluorescent material as an optical probe employ wavelength-selective sophisticated optics equipment, and this is not suitable for the portable device because of the high cost, high power consumption, and complex equipment requirement. Therefore, the development of a sensor that does not require complicated equipment for the detection of Hg^{2+} is required.

In this study, we have introduced the retroreflection principle to develop a Hg^{2+} sensor that does not require complicated instrumentation. Retroreflection is a phenomenon in which light reflected by a particular object returns to the light source. Because retroreflection is generated to various light sources including visible light and non-monochromatic light, the equipment for irradiating a specific light source (wavelength) is not required (Stoudt et al., 1978; Schultz et al., 2012). A number of studies have been reported on the application of retroreflection principle for biosensor development including retroreflector cube (Garvey et al., 2014), photo-lithographically fabricated linear microreflector (Raja et al., 2016) and retroreflective Janus microparticle (Han et al., 2016). To integrate the retroreflection principle into a Hg^{2+} sensing platform, we used retroreflective Janus microparticles (RJPs) as an optical signaling probe. It has been reported that retroreflection from RJPs is easily

induced by a common white light-emitting diode (LED) (Han et al., 2016). Since the RJPs can be observed using simple optical equipment such as a low magnification complementary metal oxide semiconductor (CMOS) camera, it is suitable for use as an optical signaling probe in portable equipment. To apply RJPs containing these features to the Hg^{2+} sensor, a T-Hg^{2+}-T base pairing-based sensing strategy using a stem-loop DNA probe was employed (Fig. 1).

<Figure 1>

The stem-loop DNA probe was labeled with an amine and a biotin at the 3′- and 5′-termini, respectively. When Hg^{2+} is not present, the stem-loop DNA probe was present as a hairpin structure. However, in the presence of Hg^{2+} and the assistant DNA probe, the stem-loop DNA was stretched by a T-T mismatch, exposing the biotin. When the streptavidin-conjugated RJPs (SA-RJPs) were added, SA-RJPs bound to the exposed biotin of the DNA probe, and reacted-SA-RJPs were observed using a simple optical apparatus. At this time, the number of SA-RJPs that reacted with the exposed biotin was proportional to the applied Hg^{2+} concentration. Therefore, Hg^{2+} could be quantitatively analyzed as a signal-on type sensor by counting the number of observed SA-RJPs. Using the developed Hg^{2+} sensing system, it was possible to sensitively and selectively measure the Hg^{2+} present in real samples, such as tap water and bottled water, as well as in the buffer. The details of the sensing system and its detection performance, including the limit of detection, sensitivity, and selectivity, are described below.

2. Experimental procedures

2.1 Materials and instruments

A biotinylated stem-loop DNA probe (5′-NH_2-$(CH_2)_6$-GTGAGC AAAGA GACCT ACCAT ACGGG CCATT TGTCT GCTCAC-$(CH_2)_2$-Biotin-3′) and an assistant DNA probe (3′-TTTCT CTGGT TGGTT TGCCC GGTTA ACTGA-5′) were synthesized and obtained from Bioneer (Daejeon, Korea). The retroreflective Janus particle-

quantifying chips (RQC) were acquired from AMED (Seoul, Korea). Streptavidin, biotinylated fluorescent beads (0.04 μm, 505/515 nm), and 3,3′-Dithiobis(sulfosuccinimidyl propionate) (DTSSP) was obtained from Thermo Scientific (Waltham, MA, USA). Mercury (II) chloride, ethanolamine (EA), tris(hydroxymethyl)amino-methane, sodium dodecyl sulfate (SDS), sucrose, arginine, tween-20 (Tw-20), triton X-100 (Tx-100), polyethylene glycol (PEG), and poly(vinyl alcohol) (PVA) were purchased from Sigma-Aldrich (St. Louis, MO, USA). Bovine serum albumin (BSA) was obtained from BioWorld (Dublin, Ohio, USA). Sodium chloride (NaCl) was obtained from Duchefa Biochemie (Haarlem, Netherlands). The storage buffer was obtained from Ademtech (Pessac, France). VZM™ 450i Zoom Imaging Lens and CMOS Color USB Camera (5 megapixels) were purchased from Edmund Optics (Barrington, NJ, USA). For the reaction solutions, reaction buffer (RBS; 10 mM Tris-HCl and 200 mM NaCl, pH 8.0), Washing buffer I (WBS I; 10 mM Tris-HCl, 200 mM NaCl and 0.1% SDS, pH 8.0), Washing buffer II (WBS II; 20 mM Tris-HCl, 1% BSA, 1% sucrose, 50 mM NaCl, 50 mM arginine, 0.2% Tw-20, 0.2 % Tx-100, 0.2% PEG, and 0.5% PVA, pH 7.4), and double distilled and deionized water (DDW).

2.2 Preparation of Streptavidin-RJP and sensing surface

To measure the concentration of Hg^{2+} using the retroreflection-based optical sensing approach, the optical signaling probe RJPs were fabricated according to the synthesis method reported in the previous study (Han et al., 2016). Briefly, to fabricate RJPs, the hemispherical surface of the silica microparticles (1.2 μm in diameter) was sequentially coated in aluminum (Al; 40 nm) and gold (Au; 20 nm) via the e-beam physical vapor deposition method. Then, the gold-coated hemispherical surface of fabricated RJPs was decorated with amine-reactive self-assembled monolayer by pouring DTSSP (5 mM) onto the RJP-deposited substrate for 3 h. After washing with DDW, 100 μg/mL streptavidin (in PBS, pH 7.2) was applied to the DTSSP-modified RJPs. During this process, streptavidin was covalently bound to the DTSSP-modified gold region of RJPs via amide bond formation between the amine groups of streptavidin and the sulfosuccinimidyl ester (sulfo-NHS) moieties of DTSSP. After washing with PBS, the unreacted sulfo-NHS groups were blocked by incubating for 30 min with 20 mM EA. A 1% BSA solution was used to block nonspecific binding to the silica region of the RJPs. Finally, the SA-RJPs deposited on the glass substrate were collected by ultra-sonication and centrifugation. The collected SA-RJPs were stored in the Ademtech storage buffer at 4°C until further use (Fig. 2(A)). As a negative

control, surface-blocked RJPs were prepared by treating with EA and BSA instead of streptavidin to DTSSP-modified RJPs. The prepared negative control RJPs were also stored in a storage buffer at 4°C.

<Figure 2>

To construct a Hg^{2+} sensing surface using DNA, the RQC was fabricated and used as a sensing surface. The RQC consists of 16 gold-patterned sensing zones (340 x 340 μm^2 in dimension), made using conventional photolithography techniques, and the thin films of chromium (30 nm) and gold (150 nm) were sequentially coated on the glass using a sputter system. First, the surface of the prepared RQC was cleaned by piranha solution for 5 minutes. After cleaning with DDW, 5 mM DTSSP was reacted on the gold region of RQC for 3 h. After washing with DDW, 10 μM stem-loop DNA probe in RBS was applied and incubated for 1 h at 40°C. At this time, to prevent self-hybridization in the DNA probe and hybridization between the DNA probes, this reaction was carried out at a 40°C. This temperature is higher than the T_m value (intra: 28, inter: 38), so that the separated DNAs could individually react with the DTSSP-modified sensing surface. Next, the sensing surface was rinsed with WBS I to remove the DNA not reacted with DTSSP. Finally, the basic preparation of Hg^{2+} sensing surface construction was completed by reacting 20 mM EA in RBS for 0.5 h to block the unreacted sulfo-NHS residues of DTSSP (Fig. 2(B)).

2.3 Measurement process of mercury ion concentration

To measure the concentration of Hg^{2+}, mixed solutions containing an assistant DNA and various concentration of Hg^{2+} were applied to the DNA probe-modified RQC and reacted for 0.5 h at 40°C. After 0.5 h, the RQC was stored for 0.5 h at 4°C so that DNA probes that did not react with assistant DNA could resume the hairpin conformation. After the RQC was washed with WBS I, 1% BSA was injected for 1 h to prevent nonspecific binding between the surface of RQC and RJPs. Next, SA-RJPs were loaded at a concentration of 0.5 mg/mL and reacted for 15 minutes. The RQC was washed with WBS II to remove SA-RJPs that did not bind to biotin or reacted with the sensing surface of RQC nonspecifically. To registered and count the RJP, which is combined with the biotin by T-T mismatch, an optical system using a white LED and CMOS camera were used as a light

source and image registering device, respectively. The result images obtained from the optical system were analyzed using the NIH ImageJ software.

2.4 Selectivity test and verification of practical possibility using real samples

To demonstrate that the developed sensor selectively reacts with Hg^{2+}, other metal ions were used as target analytes instead of Hg^{2+}. Seven metal ions (Pb^{2+}, Fe^{2+}, Ca^{2+}, Ni^{2+}, Mn^{2+}, Cu^{2+} and Zn^{2+}) were used in this experiment, each at a final concentration of 1 μM. Mixed solution I, which contains all metal ions except Hg^{2+}, and mixed solution II, which includes all metal ions including Hg^{2+}, were used to demonstrate selectivity. The experimental procedure was performed by the same method as Hg^{2+} detection, and the number of RJPs was counted by analyzing the obtained data using the ImageJ program.

To verify that the developed Hg^{2+} measurement system works on real samples as well, bottled water and tap water spiked with various concentrations of Hg^{2+} were tested. The Hg^{2+} spiked real samples were diluted 100 times with RBS, and then applied to the developed Hg^{2+} measurement system. The experimental procedure was the same as described above, and the RJP was also counted in the same method.

3. Results and discussion

3.1 Signaling principle of mercury ion detection using Hg^{2+}-mediated T-T base pairing and retroreflection

Mercury causes serious maladies in humans, including brain and kidney damage. To accurately measure mercury, a detection strategy was employed that incorporated retroreflection and the stem-loop structure-based T-T mismatch. In general, the DNA base thymine pairs with the base adenine, due to their double hydrogen bond. However, mercury can intercalate between the thymine-thymine base pair, forming the T-Hg^{2+}-T structure (Ono and Togashi, 2004; Wang et al., 2011). Based on this property, two DNA molecules were designed to alter the stem-loop structure to facilitate the binding of Hg^{2+}. First, the stem-loop DNA probe containing an amine and a biotin at the 3′- and the 5′-termini was prepared, and the complementary DNA template against the loop region of stem-loop DNA probe (assistant DNA) was synthesized.

- Stem-loop type DNA probe: 5′-GTGAGC AAAGA GACCT ACCAT ACGGG CCATT TGTCT GCTCAC-3′

- Assistant DNA: 3′-TTTCT CTGGT TGGTT TGCCC GGTTA ACTGA-5′

At this time, the four adenine bases of the assistant DNA probe were replaced with thymine bases (the underlined bases on assistant DNA). Therefore, the stem-loop DNA probe was steadily maintained as a hairpin structure in the absence of Hg^{2+} because the two DNA templates do not hybridize due to the mismatched thymine bases. However, in the presence of Hg^{2+}, the two DNA templates could hybridize due to the formation of the Hg^{2+} complex, and thus the stem-loop structure was transformed to the linear double helix, exposing biotin. To recognize the structural change of the template, streptavidin-conjugated RJPs (SA-RJPs) were employed as signaling probes. Since the RJP could retroreflect the incident light in the whole spectrum, many possible light sources could be used, and complicated spectroscopic optical analysis systems such as fluorometers and spectrometers could be effectively diminished. Therefore, because of the minimal requirements, a general white LED was employed. In the observation of RJP through the common CMOS camera, the particles were measured in the form of a dot, and the number of particles was proportional to the concentration of mercury. By counting the number of particles by using the ImageJ software, quantitative analysis was possible.

3.2 Confirmation of functionalization of RJP surface and sensing surface

In the developed Hg^{2+} sensing system, the concentration of Hg^{2+} was measured by counting the number of RJPs that can interact with the exposed biotin. For the recognition of biotin using RJPs, RJPs were conjugated with streptavidin using the methodology described in section 2.2. As the negative control, RJPs modified with bovine serum albumin (BSA) instead of streptavidin were prepared by the same manner as the preparation of SA-RJPs. To confirm streptavidin modification on the RJP surface, a fluorescence microscopic study was performed using biotinylated fluorescent beads as a signal reporter. Solutions containing 25 μg/mL biotinylated fluorescent bead were injected into 0.5 mg/mL RJP samples, including SA-RJPs and BSA-modified RJPs (control-RJPs). After reacting for 1 h, reacted particles were obtained by using centrifugation and washed with PBST (50 mM PBS, 0.01% Tw-20, pH 7.4) to remove the RJPs that did not react with fluorescent beads. The resulting images were obtained using a fluorescence microscope, and the results are shown in Fig. 3.

<Figure 3>

In the case of control-RJPs (Fig. 3(A)), the fluorescence signal was not observed. These results show that the surface of the control-RJPs was completely blocked by BSA, so that the fluorescent bead could not bind to control-RJPs. Furthermore, since the fluorescence signal was not observed at all, it can be seen that the fluorescent bead did not bind to the control-RJPs even by nonspecific adsorption. Conversely, for the SA-RJPs (Fig. 3(B)), fluorescence signals were observed in most of the particles. These results suggest that the biotinylated fluorescent bead was well coupled with the SA-RJPs, indicating that the streptavidin functionalization of RJPs was accomplished.

Next, the construction of recognition layer on RQC was confirmed. The rectangular gold patterns on RQC, where the stem-loop DNA probe was functionalized, was modified using the steps explained in section 2.2. As a negative control, BSA-modified RQC surface was also prepared and tested. A DNA sample that has perfectly complementary sequence against the loop region of the stem-loop DNA probe was treated in the surface-modified RQC. Then, the neutravidin labeled fluorescent bead was applied. These fluorescent beads could react only with the stem-loop DNA probe-immobilized RQC, because the added complementary DNA stretched stem-loop DNA probes to allow the binding between fluorescent bead and exposed biotin. Therefore, fluorescence signal could be traced to demonstrate whether stem-loop DNA probes have been successfully immobilized. As shown in Fig. S1(supporting information), distinct fluorescence signal was observed from the stem-loop DNA-modified RQC, while no fluorescence signal was detected from the BSA-modified RQC. This indicates that the stem-loop DNA has been successfully modified on the RQC, confirming the construction of recognition layer. Combining these result, we concluded that the prepared RJPs and RQC could be employed as an optical signaling probe and a sensing surface for Hg^{2+} detection.

3.3 Calibration study using developed mercury ion detection platform

To verify the feasibility of the developed optical Hg^{2+} sensing system, a T-T mismatch-based Hg^{2+} measurement assay using RJPs as an optical signaling probe was performed. In general, Hg^{2+} can be found at different concentrations in various environments, such as soil, atmosphere, and water. Among them, we focused on measuring the concentration of Hg^{2+} present in water. The US-EPA and World Health Organization (WHO)

define the maximum allowable contamination level of Hg^{2+} present in drinking water as 10 nM and 5 nM, respectively. In addition to this, the maximum allowable contamination level of Hg^{2+} in liquid industrial effluents was defined as 50 nM by the US-EPA (Teh et al., 2014; Nolan and Lippard, 2008; US-EPA., 2001). Therefore, we measured Hg^{2+} at concentrations ranging from 0 to 100 nM, which includes the maximum allowable contamination level of the Hg^{2+} present in drinking water and liquid industrial effluents. Each sample contained Hg^{2+} at various concentrations mixed with assistant DNA, and were injected into the stem-loop DNA probe-immobilized RQC. The RQC were incubated for 30 minutes at 40°C. (Fig. 4(A)).

<Figure 4>

During the reaction process, the stem-loop DNA probes are stretched by injected assistant DNA and Hg^{2+} due to the T-T mismatch, exposing biotin to the outside. At this time, since the reaction temperature is higher than the T_m of the stem region, it is possible that the DNA probe is spread out, but not due to the T-T mismatch. In this case, regardless of the concentration of Hg^{2+}, all of the SA-RJPs would react with the exposed biotin, and the maximum signal would be observed. Therefore, to restore the unreacted stem-loop DNA probes to the hairpin structure again, RQCs were incubated for 30 minutes at 4°C after the reaction process. Then, to prevent nonspecific binding, RQCs were blocked with 1% BSA for 1 hour before reacting with SA-RJP for 15 minutes. After rinsing with WBS II, the images of the resulting Hg^{2+} sensing surface of RQC were observed and registered using an optical imaging setup consisting a white LED and CMOS digital camera. The white LED and CMOS camera were installed above the sensing surface, and to selectively obtain only the result of the light by the retroreflection, the incident angle of the white LED light toward the sensing surface was fixed at 70°. The CMOS camera was connected to a computer, so that the sensing surface could be digitally registered as image files during the measuring process (Fig. 4(B)) (Han et al., 2016). As shown in Fig. 4(B), the number of observed shining dots was increased in accordance with the increase in Hg^{2+} concentration. Since the RJPs could retroreflect the light of a white LED, the shining dots could be regarded as RJPs, after binding the exposed biotin by the T-T mismatch. To accurately count the number of RJPs responding to Hg^{2+} concentration, the number of observed shining dots was counted by using the NIH ImageJ program (Fig. 4(C)). In the results using ImageJ program, the number of residual RJPs observed at 0, 0.1, 1, 10, and 100 nM Hg^{2+} conditions are shown

in Fig. 4(C). About 40.3 RJPs were observed when the Hg^{2+} concentration was 0 nM, and this value was considered to be the background signal observed due to nonspecific binding between the RQC and RJPs. To demonstrate the reproducibility of the background signal, the same experiment was conducted at least three times, and the standard deviation value of the mean was calculated to be about 10%. These results indicate that the developed system has a constant background signal. In the Fig. 4(C), the bars in the graph steadily increased in proportion to the increase in Hg^{2+} concentrations, indicating the dynamic range of the assay. Fig. 4(D) presents the calibration curve for Hg^{2+} sensing, demonstrating the gradual increase in the number of observed RJP with increasing Hg^{2+} concentrations. Based on the obtained calibration curve, the LOD was 0.027 nM, calculated by using the method suggested by Armbruster (Armbruster and Pry, 2008). Because the calculated LOD value is lower than the allowed concentration of Hg^{2+} in drinking water provided by US-EPA and WHO (10 nM), the analytical performance of the developed optical-based Hg^{2+} sensing system employing the T-T mismatch satisfies this requirement for the detection of Hg^{2+}. Based on these results, the sensing system can successfully perform quantitative analysis of Hg^{2+} in drinking water, employing the simple white LED and low magnification CMOS camera system. A number of studies have been reported on the Hg^{2+} detection by using Hg^{2+}-mediated T-T base pairing. Detection principles employed, sensing materials and reported LOD values were compared, showing the utility of the developed strategy by integrating the Hg^{2+}-mediated T-T base pairing and RJP (Table S1, supporting information).

3.4 Verifying the selectivity of the developed mercury ion sensing system for the mercury ion

In the developed Hg^{2+} sensing system, the signal would be observed when the hairpin structure was unfolded by the T-T mismatch. In the prior experiments the T-T mismatch was induced only in the presence of Hg^{2+}. Therefore, to demonstrate that other metal ions do not also unfold the hairpin structure, the specificity of the test was evaluated. Various solutions containing divalent metal ions (Pb^{2+}, Fe^{2+}, Ni^{2+}, Ca^{2+}, Mn^{2+}, Cu^{2+}, and Zn^{2+}) were prepared at a 1 μM concentration, respectively, and were applied to the stem-loop DNA probe modified RQC. Mixed solution I (all metal ions except Hg^{2+}) and mixed solution II (all metal ions including 1 nM Hg^{2+}) were analyzed, and the experimental procedure was carried out in the same conditions as before.

<Figure 5>

Fig. 5 shows the results obtained by applying the prepared solutions to the sensing system. Registered RQC image data are shown in the Fig. S2 (supporting information). In the control solution with no metal ions, the number of observed RJPs was similar to the background signal measured previously. In the Fig. 5, a large number of RJPs were observed in mixed solution II containing Hg^{2+}. However, in the solutions in which Hg^{2+} was not present, the measured signal was very little, even though the concentration of metal ions were about 1,000 times higher than the Hg^{2+} in mixed solution II. These results clearly show that the developed optical Hg^{2+} sensing system is not sensitive to other metal ions, and has excellent selectivity for Hg^{2+} detection, demonstrating that the hairpin structure was not stretched by other metal ions.

3.5 Recovery test of mercury ion in real water samples

Through the previous results, it has been demonstrated that the developed Hg^{2+} sensing platform has high sensitivity and selectivity in the tested buffer conditions. However, to be used as a Hg^{2+} sensor, it is necessary to be able to detect not only the Hg^{2+} present in the artificial buffer sample but also the Hg^{2+} present in real samples. Therefore, to evaluate the applicability of the developed Hg^{2+} sensor to real samples, commercial bottled water and tap water were tested. Each sample was spiked with various concentration of Hg^{2+} (0, 5, 20, and 50 nM) and these samples were diluted 100-fold with RBS. These prepared sample solutions were analyzed using the developed sensing platform, and the results are summarized in Table 1.

< Table 1>

For solutions with 0 nM Hg^{2+}, the counted number of RJPs in the bottled water and tap water were 39.5 and 40.6, respectively. This value is similar to the background signal. These results indicated that both samples have no material that interferes with the detection of Hg^{2+}, so the developed sensing platform could be used for this type of sample. From Table 1, in the case of bottled water, the numbers of counted RJPs for the added Hg^{2+} concentrations of 5, 20, and 50 nM are 78.8, 107.2, and 130.9, respectively. The Hg^{2+} concentrations were

estimated using the previously obtained calibration curve, and were 5.6, 21.1, and 54.8 nM, respectively. The Hg^{2+} concentrations in tap water were calculated in the same way. The recoveries were calculated by using the formula given below in Table 1, the values of which are listed in Table 1. The result of Table 1 indicated that the recoveries of the developed Hg^{2+} sensor is satisfactory because the recovery was calculated within 10%. Based on these results, we concluded that the developed Hg^{2+} sensor has the ability to detect Hg^{2+} in real environmental water samples.

4. Conclusions

We developed an optical Hg^{2+} sensing platform based on a T-T mismatch by using RJPs as an optical signaling probe. Compared with the existing detection systems for Hg^{2+} using fluorescent materials as an optical probe, the developed Hg^{2+} sensing system was able to detect Hg^{2+} without complicated optical equipment, since the property of RJP which reflects all light and can be observed with the simple optical system. Using this system, Hg^{2+} could be detected with an LOD of 0.027 nM, which is lower than the upper limit for Hg^{2+} concentration in drinking water. Moreover, the developed system not only had high selectivity but also confirmed that it could be applied to real samples. Based on the results of this study, our developed analytical system is a promising technology for DNA-based Hg^{2+} monitoring in real environments.

Acknowledgements

This research was mainly supported by Samsung Research Funding Center of Samsung Electronics under Project Number SRFC-IT1401-51. H.Y. acknowledges the support from the National Research Foundation of Korea (NRF-2016R1A2B4006564).

References

Armbruster, D.A., Pry, T., 2008. Clin. Biochem Rev. 29, S49–S52.

Bloom, N., Fitzgerald, W.F., 1988. Anal. Chim. Acta 208, 151–161.

EPA, U.S., 2001. Mercury Update: Impact on Fish Advisories. In: EPA, U.S. (Ed.), EPA-823-F-01-011.

Ferrua, N., Cerutti, S., Salonia, J.A., Olsina, R.A., Martinez, L.D., 2007. J. Hazard. Mater. 141 (2), 693–699.

Fong, B.M.W., Siu, T.S., Lee, J.S.K., Tam, S., 2007. J. Anal. Toxicol. 31 (5), 281–287.

Garvey, G., Shakarisaz, D., Ruiz-Ruiz, F., Hagstrom, A.E.V., Raja, B., Pascente, C., Kar, A., Kourentzi, K., Rito-Palomares, M., Ruchhoeft, P., Willson, R.C., 2014. Anal. Chem. 86 (18), 9029-9035.

Han, Y.D., Kim, H-S., Park, Y.M., Chun, H.J., Kim, J-H., Yoon, H.C., 2016. ACS Appl. Mater. Interfaces 8, 10767-10774.

He, X., Qing, Z., Wang, K., Zou, Z., Shia, H., Huanga, J., 2012. Anal. Methods 4, 345-347.

Hou, P., Long, Y., Zhao, J., Wang, J., Zhou, F., 2012. Spectroc. Acta Pt. A-Molec. Biomolec. Spectr. 86, 76-79.

Huang, J.H., Gao, X., Jia, J.J., Kim, J.K., Li, Z.G., 2014. Anal. Chem. 86, 3209–3215.

Kim, I.-B., Bunz, U.H., 2006. J. Am. Chem. Soc. 128 (9), 2818–2819.

Lee, J.S., Han, M.S., Mirkin, C.A., 2007. Angew. Chem. Int. Ed. 46, 4093–4096.

Li, L., Wen, Y., Xua, L., Xu, Q., Song, S., Zuo, X., Yan, J., Zhang, W., Liu, G., 2016. Biosens. Bioelectron. 75, 433–445.

Li, Y., Jiang, Y., Yan, X-P., 2006. Anal. Chem. 78, 6115-6120.

Li, Y.K., Xu, Y.R., Huang, Y., Dai, Y., Hu, Q.F., Yang, G.Y., 2009. Chem. Asian J. 21, 2893–2897.

Liu, J., Lu, Y., 2007. Angew. Chem. Int. Ed. 46 (40), 7587–7590.

Lu, M.H., Xiao, R., Zhang, X.N., Niu, J.H., Zhang, X.T., Wang, Y.M., 2016. Biosens. Bioelectron 85, 267–271.

Lv, X., Wu, W., Niu, C., Huang, D., Wang, X., Zhang, X., 2016. Talanta 151, 62–67.

Malinovsky, D., Sturgeon, R.E., Yang, L., 2008. Anal. Chem. 80 (7), 2548–2555.

Miller, J.R., Rowland, J., Lechler, P.J., Desilets, M., Hsu, L.C., 1996. Water Air Soil Pollut. 86, 373–388.

Nolan, E.M., Lippard, S.J., 2008. Chem. Rev. 108, 3443–3480.

Ono, A., Togashi, H., 2004. Angew. Chem. Int. Ed. 43, 4300–4302.

Raja, B., Pascente, C., Knoop, J., Shakarisaz, D., Sherlock, T., Kemper, S., Kourentzi, K., Renzi, R.F., Hatch, A.V. Olano, J., Peng, B-H., Ruchhoeft, P., Willson, R.C., 2016. Lab Chip 16, 1625-1635.

Ros-Lis, J.V., Marcos, M.D., Mártinez-Máñez, R., Rurack, K., Soto, J., 2005. Angew. Chem. Int. Ed. 44 (28), 4405–4407.

Rurack, K., Resch-Genger, U., Bricks, J. L., Spieles, M., 2000. Chem. Commun. 21, 2103–2104.

Schultz, P., Cumby, B., Heikenfeld, J., 2012. Appl. Optics 51, 3744−3754.

Stoudt, M.D., Vedam, K., 1978. Appl. Optics 17, 1855−1858.

Tao, Y., Lin, Y.H., Ren, J.S., Qu, X.G., 2013. Biomaterials 34, 4810–4817.

Teh, H.B., Wu, H., Zuo, X., Li, S. F. Y., 2014. Sens. Actuators B-Chem. 195, 623–629.

Wang, G., Lu, Y., Yan, C., Lu, Y., 2015. Sens. Actuators B-Chem. 211, 1–6.

Wang, L., Tian, J., Li, H., Zhang, Y., Sun, X., 2011. Journal of Fluorescence 21 (3), 1049–1052.

Wang, Y., Geng, F., Cheng, Q., Xu, H., Xu, M., 2011. Analyst 136, 4284-4288.

Wegner, S.V., Okesli, A., Chen, P., He, C., 2007. J. Am. Chem. Soc. 129 (12), 3474–3475.

Wordofa, D.N., Ramnnani, P., Tran, T.T., Mulchandani, A., 2016. Analyst 141, 2756–2760.

Xiong, E., Wu, L., Zhou, J., Yu, P., Zhang, X., Chen, J., 2014. Anal. Chim. Acta 2015, 242-248.

Xu, H., Zhu, X., Ye, H., Yu, L., Liu, X., Chen, G., 2011. Chem. Commun. 47, 12158-12160.

Yang, K., Zeng, M., Hu, X.J., Guo, B.S., Zhou, J.B., 2014. Analyst 139, 4445–4448.

Yang, Y., Jiang, J., Shen, G., Yu, R., 2009. Anal. Chim. Acta 636 (1), 83–88.

Yang, Y.K., Yook, K.J., Tae, J., 2005. J. Am. Chem. Soc. 127 (48), 16760–16761.

Yao, L., Teng, J., Zhu, M.Y., Zheng, L., Zhong, Y.H., Liu, G.D., Xue, F., Chen, W., 2016. Biosens. Bioelectron. 85, 331–336.

Yu, Z.G., Lai, R.Y. 2012. Chem. Commun. 48, 10523-10525.

Zhang, L. Chang, H.X., Hirata, A., Wu, H.K., Xue, Q.K., Chen, M.W., 2013. ACS Nano 7, 4595–4600.

Zhao, X., Gao, J.S., He, L., Cong, L.C., Zhao, H.M., Li, X.Y., Tan, F., 2015. RSC Adv. 5, 39587–39591.

Zhou, Z., Huang, H., Chen, Y., Liu, F., Huang, C.Z., Li, N., 2014. Biosens. Bioelectron. 52, 367–373.

Zuo, X.W., Zhang, H.G., Zhu, Q., Wang, W.F., Feng, J., Chen, X.G., 2016. Biosens. Bioelectron. 85, 464–470.

Figure captions

Figure 1. Scheme of the principles used in the developed optical biosensing system based on the T-T mismatch. In the presence of Hg^{2+} and the assistant DNA, the stem-loop DNA probe was unfolded, exposing the biotin. Then, streptavidin-conjugated RJPs could be bound to the exposed biotin. The number of SA-RJPs interacting with biotin could be measured by employing the simple optics system.

Figure 2. Workflows of the functionalization procedures for SA-RJPs (A) and the construction process of Hg^{2+} recognition layer on the gold-modified surface of RQC (B).

Figure 3. Fluorescence microscopy images of SA-RJP and control-RJPs after the labeling with biotinylated fluorescent beads. Fluorescence signal was not observed in control-RJPs (A). However, large amounts of fluorescence signals were observed for SA-RJPs (B).

Figure 4. (A) A schematic of the process by which the optical probe SA-RJPs combine with exposed biotin. This process occurs only when the stem-loop DNA probe is present in the form of a linear double helix due to mercury ions. (B) The resulting images of the Hg^{2+} measurement assay for various Hg^{2+} concentrations (0, 0.1, 1, 10, 100 nM) by using the developed sensing system. The images were digitally registered by employing a simple imaging setup, such as white LED and CMOS digital camera. (C) A graph showing the number of observed RJPs in the resulting images. The RJPs were quantitatively analyzed using the ImageJ program. (D) The calibration curve for the Hg^{2+} detection assay. The assay was performed three times, and the error bars indicate the standard deviations.

Figure 5. The selectivity of the developed Hg^{2+} sensing platform. A total of 10 solutions were analyzed. The final concentration of Hg^{2+} in the solution was 1 nM and the other metal ions were 1 μM. Despite the presence of metal ions at 1,000 times the concentration of mercury ions, significantly lower signals were observed than in solutions in which mercury ions were present.

Figure 1

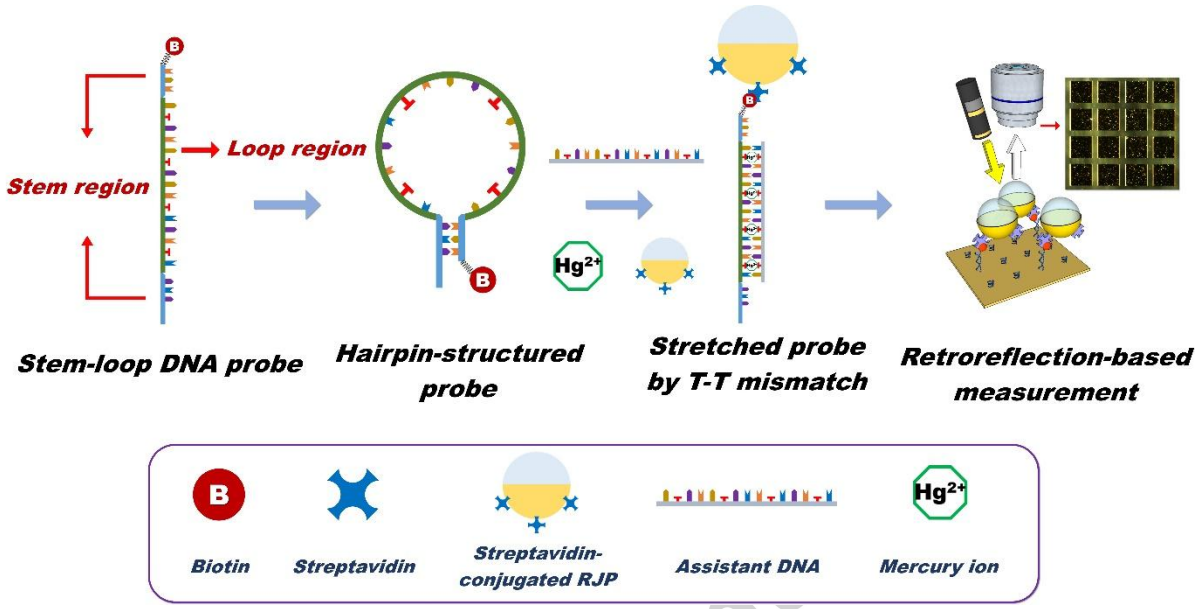

Figure 2

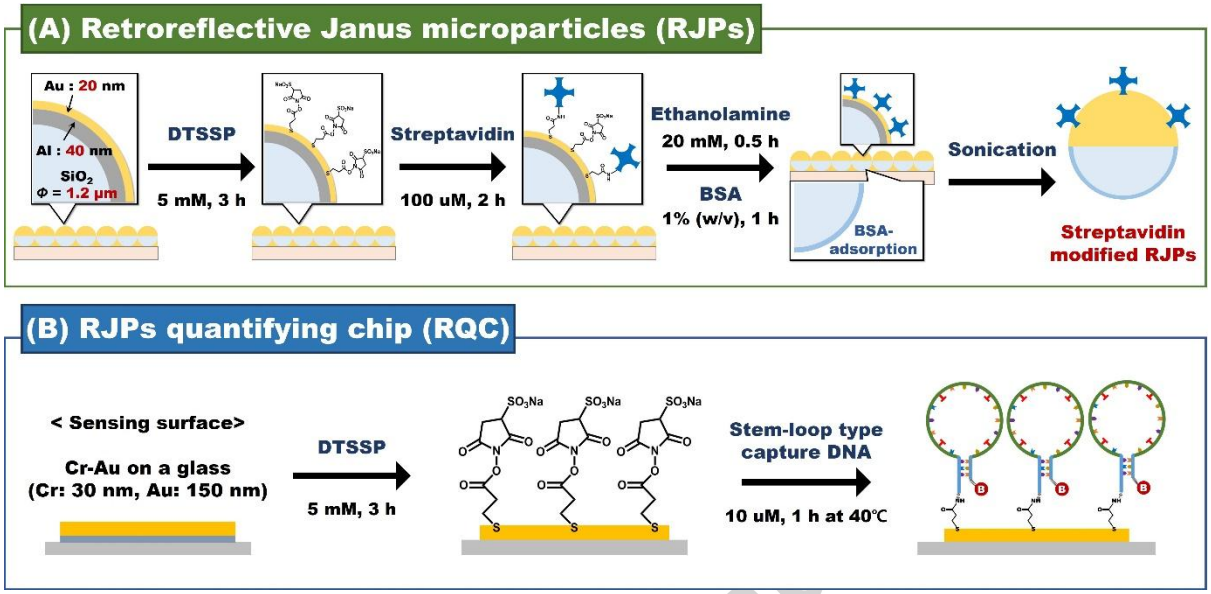

Figure 3

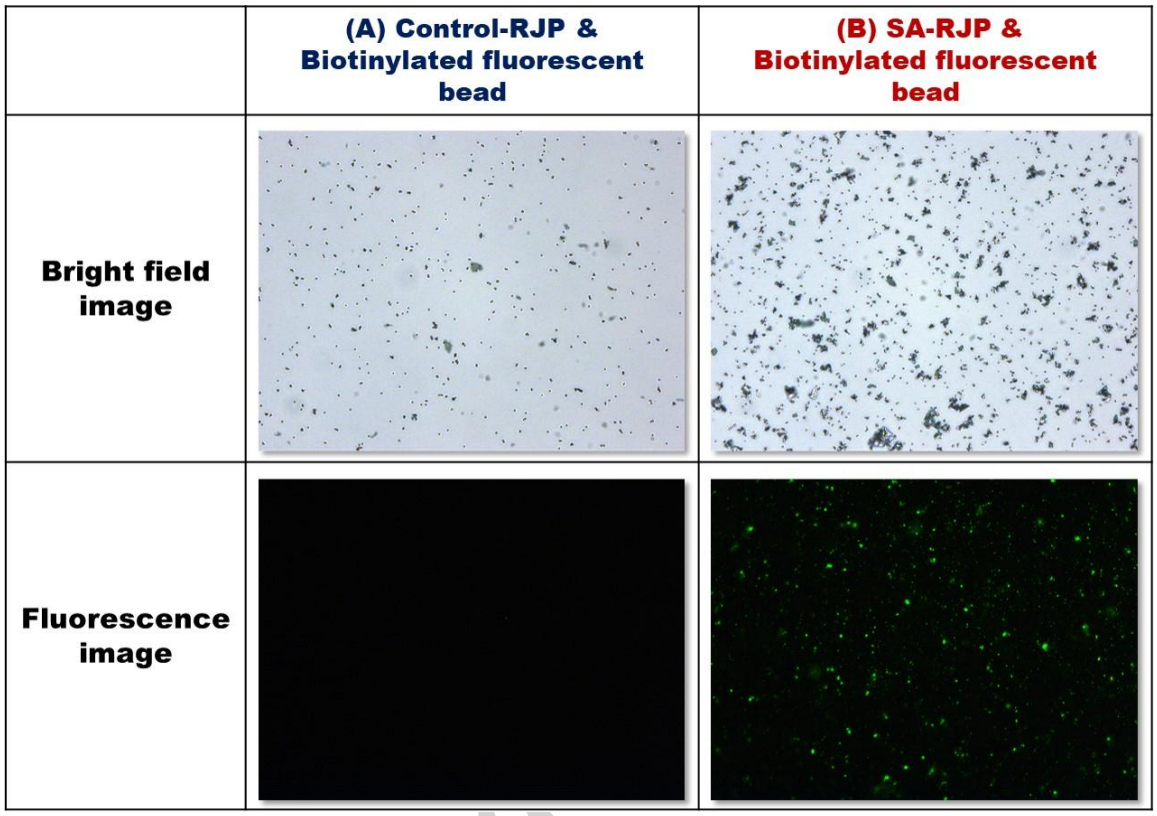

Figure 4

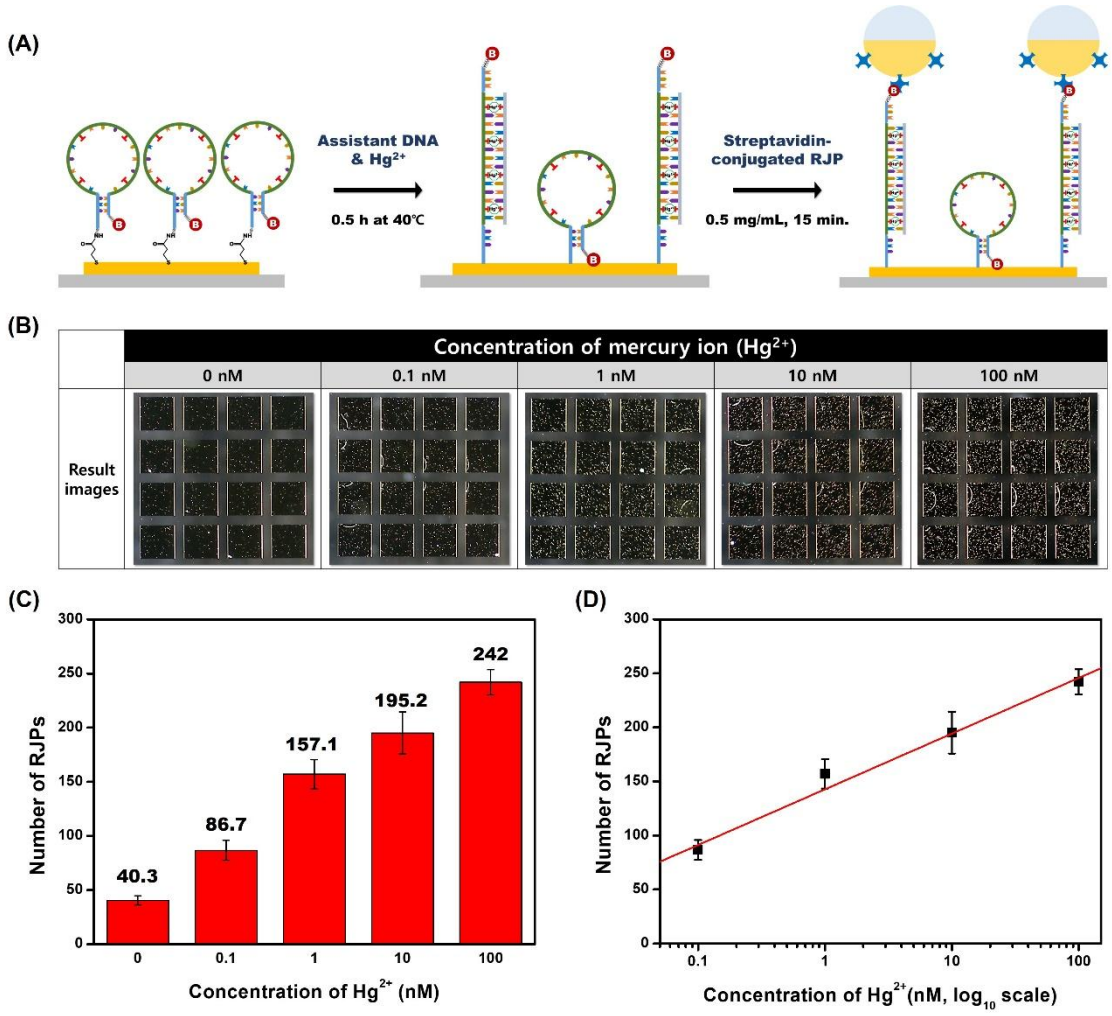

Figure 5

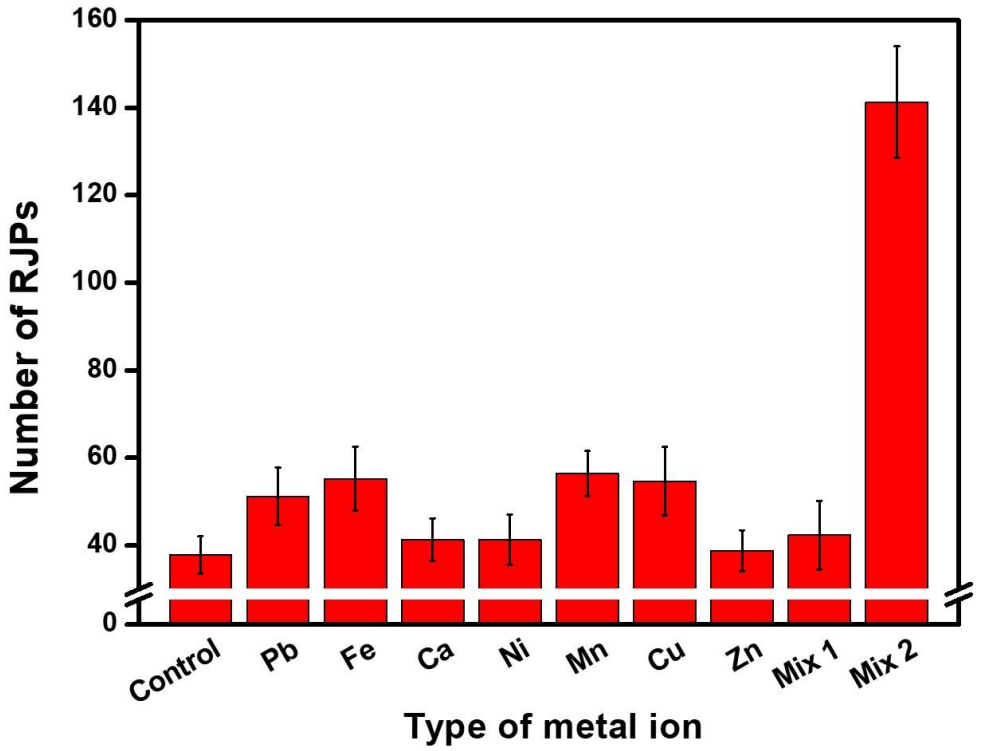

Table 1

Table 1. Recovery assays of Hg^{2+} in real water samples using the developed sensing platform.

Sample	Added Hg^{2+} (nM)	Number of RJPs	Found Hg^{2+} (nM)	Recovery (%)
Bottle water	0	39.5 ± 4.5	< 0.1	-
	5	78.8 ± 15.5	5.6	112.0
	20	107.2 ± 13.3	21.1	105.5
	50	130.9 ± 16.6	54.8	109.6
Tap water	0	40.6 ± 4.0	< 0.1	-
	5	73.9 ± 11.6	4.9	98.0
	20	104.7 ± 10.1	18.5	92.5
	50	124.7 ± 8.4	47.2	94.4

Recovery (%) = Found Hg^{2+} (nM) / Added Hg^{2+} (nM) × 100

Highlights

- Retroreflection-based mercury ion sensing strategy was developed.
- Hg^{2+}-mediated thymine-thymine (T-T) pairing was employed as Hg^{2+} sensing principle.
- Retroreflective Janus particle was utilized as an optical signaling probe for Hg^{2+} detection.
- Retroreflection-based Hg^{2+} sensing system enables accurate, convenient and cost-effective Hg^{2+} detection
- Hg^{2+} sensor showed linear dynamic range between 0 to 100 nM with the detection limit of 0.027 nM.